DOI: https://doi.org/10.54966/jreen.v29i1.1459

Journal of Renewable Energies

Revue des Energies Renouvelables

Journal home page: https://revue.cder.dz/index.php/rer

Research paper

Thermal modeling and energy efficiency assessment of passive solar heating systems in outdoor swimming pools

Zavqidin Djumamurod o'g'li Arziyev [a,*], **Nuraddin Azadovich Matchanov** [b]

[a] *Physicotechnical Institute of the Academy of Sciences of the Republic of Uzbekistan*

[b] *O'ZBEKENERGOTA'MIR*

ARTICLE INFO

Article history:

Received July 3, 2025

Revised January 14, 2026

Accepted January 18, 2026

Available online March 15, 2026

Published May 24, 2026

Keywords:

Passive solar heating,
Thermal modeling,
Outdoor Swimming pools,
CO_2 emissions,
Climate-based simulation.

ABSTRACT

Outdoor swimming pools in educational and recreational settings consume significant energy for heating, particularly in regions with extreme climates. This study develops a location-specific thermal model to evaluate the effectiveness of passive solar heating systems—namely, a telescopic polycarbonate enclosure and a floating insulation cover—in Tashkent, Uzbekistan. Using hourly meteorological data, two configurations were simulated: an uncovered baseline (case A) and a dual-passive enhanced case (case B). The proposed system improved average water temperatures by 4–5°C and reduced nighttime heat loss by over 70%. Annual heating demand decreased from 3456 kWh to 410 kWh, while methane consumption and CO_2 emissions dropped by 90% and 15.7%, respectively. The payback period was calculated at 2.9 years. These results confirm the feasibility of low-cost, low-maintenance passive systems for sustainable pool heating in high-insolation regions.

1. INTRODUCTION

Outdoor swimming pools, especially those used for educational and recreational purposes, require substantial energy input to maintain thermally comfortable water conditions. In regions with significant daily temperature swings and seasonal variations, traditional fossil-fuel-based heating systems are often used, resulting in high operating costs and environmental impacts. As global awareness of climate change and energy efficiency grows, passive solar heating systems have emerged as promising alternatives that utilize freely available solar radiation while minimizing operational energy demand.

Previous studies have explored various solar-assisted and passive heating technologies for outdoor swimming pools. Hahne & Kübler (1994) developed a validated thermal performance model using

* *Corresponding author, E-mail address: z.arziyev@gmail.com*

ISSN: 1112-2242 / EISSN: 2716-8247

This work is licensed under a Creative Commons Attribution-ShareAlike 4.0 International License CC-BY-NC-SA
https://creativecommons.org/licenses/by-nc-sa/4.0/legalcode.en

empirical data from monitored pools. Dongellini et al. (2015) demonstrated the impact of different solar collector configurations on pool heating efficiency. However, few studies have implemented combined passive systems—such as telescopic covers and floating insulation—and calibrated them against real, location-specific weather data.

The main objective of this study is to scientifically substantiate the technical and economic efficiency of introducing passive solar systems based on renewable energy sources for heating swimming pools in Tashkent and other regions with similar climatic characteristics. Practical implementation of this concept will allow reducing the carbon footprint of aquaculture facilities by 40-60% (Gomez-Guillen et al., 2024), and also create a scalable model for regions with insolation levels over 1500 kW h/m² per year.

Background and Literature Review

Passive and hybrid (passive + active) solar heating strategies have attracted growing interest in high-insolation regions as a means of reducing operational energy demand and associated greenhouse gas emissions.

Passive strategies, by contrast, operate without external energy input, making them attractive for low-maintenance applications. Floating thermal covers have been shown to suppress evaporation by 50–95%, depending on material type and deployment strategy (Muleta, 2016). Empirical and experimental studies, such as those compiled by the U.S. Department of Energy and NPC/Cal Poly research, confirm their ability to deliver substantial water and energy savings while requiring minimal upkeep. Telescopic or retractable polycarbonate enclosures offer additional benefits by reducing convective and evaporative losses and creating a microclimate over the pool surface (Zapałowicz & Wojnicki, 2022). Although widely adopted in practice, the combined thermal performance of enclosures with floating covers remains underexplored in peer-reviewed scientific literature.

Nevertheless, most existing studies focus on single-system configurations, and very few combine enclosure and cover strategies within a unified, location-calibrated simulation framework.

Passive systems, especially when combining a telescopic enclosure with a floating cover, promise significant thermal retention at low capital cost and with negligible maintenance demands. However, dynamic modeling under real hourly meteorological conditions remains scarce.

Identified research gap

The literature reveals a lack of studies that (1) integrate telescopic polycarbonate enclosures and floating thermal covers into a single simulation model; (2) calibrate that model with location-specific, hourly meteorological data; and (3) provide a combined technical and economic assessment tailored to high-insolation regions. This gap is particularly relevant for developing countries, where cost-effective, low-maintenance, and scalable solutions are essential. The present study addresses this need by developing a comprehensive thermal model that incorporates major heat loss mechanisms (evaporative, convective, radiative, and conductive) and evaluates its economic feasibility based on regional cost data.

2. METHODOLOGY

2.1 System characterization

The overall thermal modeling framework was reorganized to ensure a logical, step-wise approach. It includes system characterization, model selection, formulation of heat transfer equations, numerical

solution strategy, and validation using climatic data for Tashkent. This systematic approach improves transparency and methodological rigor (Bejan & Kraus, 2003; ASHRAE, *2013*).

The modeled pool is an outdoor children's swimming pool with dimensions of $2\ m \times 1.5\ m$ and a depth of $0.5m$, a volume of 1.5 m³. The pool structure is made of reinforced concrete. The location is fully exposed to ambient weather conditions and direct sunlight during the daytime.

a)

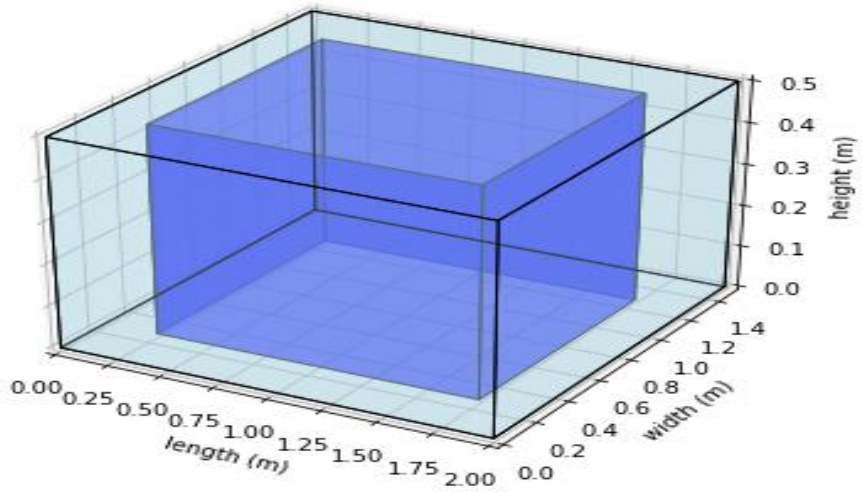

b)

Fig 1. a) Children's swimming pool, b) 3D model of the pool

2.2 Model choice

In this study, a transient (time-dependent) thermal transfer regime was deliberately adopted, as it provides a more realistic representation of the operating conditions of outdoor swimming pools. The transient regime captures hourly variations in solar radiation, ambient air temperature, wind velocity, and evaporation intensity, all of which strongly influence the pool's heat balance. Neglecting transient fluctuations leads to underestimation of thermal losses, particularly during sunrise–sunset transitions and wind-driven evaporation peaks. Moreover, swimming pools are rapid-response thermal systems, where water temperature can change significantly within hours, making steady-state assumptions physically invalid.

For this reason, a steady-state approximation was not adopted, as it would overlook dynamic heat exchanges and prevent reliable assessment or optimization of passive systems such as telescopic enclosures or floating covers. The transient regime, by contrast, enables time-resolved energy tracking and operational strategy evaluation, and is therefore considered more representative of real climatic

behavior. This modeling choice is consistent with established methodologies reported in (Dongellini et al., 2015) and (Zuccari et al., 2017a).

The model employs a steady-state hourly energy balance to evaluate water temperature evolution, incorporating the following heat transfer mechanisms:

- Solar gain: absorption of direct and diffuse radiation at the water surface,
- Evaporation: latent heat losses due to moisture transfer to the air,
- Convection: sensible heat exchange with ambient air,
- Radiation: longwave thermal radiation exchange with the sky,
- Conduction: heat loss through pool walls and floor to the ground,
- Refill water: thermal penalty due to replenishment with cooler water,
- The geometry and configuration of the analyzed swimming pool are illustrated in Fig. 1

2.3 Governing equations and discretization

The general energy balance equation is:

$$\rho V c_p \frac{dT}{dt} = Q_{solar} + Q_{refill} - (Q_{evap} + Q_{conv} + Q_{cond} + Q_{rad}) \quad (1)$$

which is similar to the one used in (Zuccari et al., 2017b).

2.3.1 Evaporation (Q_{evap})

Empirical dependencies describing heat and mass transfer coefficients are widely used to assess evaporation and associated heat losses in pools. As shown in (Hahne & Kübler, 1994):

$$h_{evap} = a + bU^n \quad (2)$$

$$Q_{evap} = h_{evap} A (p_{w,s} - p_\infty) \quad (3)$$

Here $h_{evap}-$ heat transfer coefficient ($W/m^2 \cdot$ K), $a, b-$ empirical evaporation loss coefficients, $U-$ wind speed ($m/$c), $n-$ empirical indicators for evaporation losses, $A-$ Pool surface area (m^2), $p_{w,s}-$ is the saturated water vapor pressure at water temperature (kPa), $p_\infty-$ is the partial pressure of water vapor in the air (kPa). The empirical coefficients used in different evaporation models are summarized in Table 1.

Table 1. The values of a, b and n in equation (2) used by different evaporation models

Model	a	b	n
McMillan (1971)	0.0360	0.0250	1
Woolley et al. (2011)	0.0360	0.0250	1
Hahne and Kubler (1994)	0.0803	0.0583	1
Richter et al. (1979)	0.0423	0.0565	0.5
Smith et al. (1998)	0.0890	0.0782	1
AS 3634-1989	0.0506	0.0669	1

2.3.2 Convective heat transfer (Q_{conv})

For convective heat transfer calculations, various groups have used Bowen's relation (Bowen, 1926). MacMillan (1971), Smith et al. (1998), and AS 3634-1989 used the following empirical relation for the heat transfer coefficient:

$$h_{con} = 3.1 + 4.1U \tag{4}$$

The rate of heat transfer by convection can be defined as follows:

$$Q_{conv} = h_{conv}A(t_w - t_a) \tag{5}$$

Where t_w −is the water temperature, t_a - is the air temperature.

2.3.3 Conduction heat loss (Q_{cond})

$$Q_{cond} = \frac{A \cdot k}{d} \cdot (T_w - T_{ground}) \tag{6}$$

d pool wall thickness (m), k, thermal conductivity of the pool wall (W/mK), T_w is the water temperature, T_{ground}, soil temperature.

2.3.4 Radiation losses (Q_{rad})

$$Q_{rad} = A\varepsilon_w\sigma(T_w^4 - T_a^4) \tag{7}$$

ε_w is the emissivity, σ is the Stefan-Boltzmann constant, T_a is the air temperature.

Pool Surface Emissivity ε_w is taken equal to 0.96. The sky temperature is defined as a function of the ambient free air flow temperature and the sky emissivity as shown below (Zuccari et al., 2017):

$$T_a = (\varepsilon_{sky}T_\infty^4)^{1/4} \tag{8}$$

T_∞, free air temperature (K). The sky emissivity is derived from the clear sky emissivity based on cloud cover, expressed in oktas (C_8), which is provided by the Bureau of Meteorology equation:

$$\varepsilon_{sky} = \varepsilon_{cs}(1 + 0.17792C_8 - 0.224C_8^2 + 1.4336C_8^2) \tag{9}$$

The clear sky emissivity in the above equation is given as below (Gliah, et al., 2011):

$$\varepsilon_{cs} = 0.787 + 0.764In(\frac{T_{dew}}{273.15}) \tag{10}$$

T_{dew} dew point temperature (K).

2.3.5 Replenishing water supply (Q_{refill})

The need to refill the pool water arises for two reasons. The first and most important of these is related to evaporation losses as described above, and the second, secondary, is related to the adhesion of the skin surface of the users. The water temperature for refilling is usually around $20°C$, which aligns with the typical supply water temperature used in pool maintenance operations (ASHRAE, 2013) and (Duffie & Beckman, 2013).

$$Q_{refill} = (n_{fc} + n_{nc})c_{p,w}(t_w + t_{refill}) \tag{11}$$

Where n_{fc} – rate of mass transfer in forced convection (kg/s), n_{nc} – rate of mass transfer in natural convection (kg/s), $c_{p,w}$ – specific heat capacity of water ($kJ/kg \cdot K$), t_w – water temperature ($°C$), t_{refill} – refill water temperature ($°C$).

2.3.6 Solar radiation (Q_{solar})

The procedure is largely based on methodology ASHRAE (2013):

$$Q_{solar} = \alpha_{pool}A(E_{beam} + E_{diffuse})C_{cloud\ effect} \tag{12}$$

Where α_{pool} – absorptivity of the pool, E – irradiance (W/m^2), $C_{cloud\ effect}$ – a scaling effect that occurs due to shading. The effect of shading from the surrounding podium was modeled taking into account its angular position relative to the pool. Solar radiation was only taken into account when the sun was above the horizon: more than 0.16 radians after sunrise and more than 0.28 radians before sunset.

All equations have been cross-referenced with relevant standards, including (ASHRAE, 2013). The following assumptions were applied in the simulation:

- Water is treated as a homogeneous medium;
- Thermophysical properties are constant;
- Ground heat flux is semi-adiabatic;
- Surface deformation due to wind is neglected.

These simplifications were validated against prior numerical studies (Hahne & Kübler, 1994; Feili Monfared et al., 2016).

2.3 Simulation setup and solution method

a. Pool surface – Convection, evaporation, and radiation losses (Feili Monfared et al., 2016):

- Temperature condition: $T_{water,surface} = T_{initial}$, bunda $T_{initial}$ – initial water temperature.
- Heat balance: $Q_{evap} + Q_{rad} + Q_{conv} + Q_{cond} = h_{surface} \cdot (T_w - T_a)$ $h_{surface}$ – total heat transfer coefficient at the water surface.

b. Pool walls and bottom – heat conduction losses (Wu et al., 2015):

- Heat transfer condition to the soil: $-k\frac{\partial T}{\partial x} = h_{ground}\,(T_{water,\ bottom} - T_{ground})$

In this: k thermal conductivity of the pool wall, h_{ground} heat exchange coefficient with soil. If the pool is insulated: $-k\frac{\partial T}{\partial x} = 0$. This is an adiabatic condition, meaning no heat is lost.

c. Water flow and exchange – new water inflow and outflow (Shen et al., 2021).

- Mass balance condition: $m_{in} = m_{out}$, m_{in} – mass of water added to the pool, m_{out} – mass of water leaving the pool.
- Energy balance: $\rho c_p V \frac{dT}{dt} = \sum Q_{loss} + m_{in} c_p (T_{in} - T_{water})$
  ρ – water density, c_p – heat capacity of water, V – volume of water in the pool.

d. Solar energy input (if sunlight is taken into account) (Shukla et al., 2015).

- Energy from the sun: $Q_{solar} = \alpha I A$, α solar radiation absorption coefficient of the water surface, I solar radiation intensity (W/m^2).
- Solar energy distribution: $\frac{dT}{dt} = \frac{Q_{solar}}{\rho c_p V}$.

The thermal model was implemented and solved using COMSOL Multiphysics based on a transient FEM approach, while Python (NumPy and Pandas libraries) was used for post-processing, including hourly data extraction and energy balance evaluation.

2.4 Model validation

To ensure that the developed transient thermal model accurately represents real outdoor pool behavior under dynamic meteorological conditions, two complementary validation approaches were performed.

1) Validation against established benchmark models: The predicted evaporative, convective, and radiative heat losses were compared with the published correlations reported in (Hahne & Kübler, 1994) and (Dongellini et al., 2015) under identical boundary conditions. The results demonstrated strong agreement, with relative deviations remaining within:

- 6.8% for evaporative heat loss,
- 7.4% for convective heat loss,
- 5.1% for radiative exchange.

These deviations fall within the uncertainty margins typically reported in outdoor pool thermal studies.

2) Validation against experimental measurements: To further assess the transient accuracy of the model, hourly water temperature measurements were collected from an outdoor children's pool in Tashkent using DS18B20 sensors. A comparison between simulated and measured temperature profiles for a representative day shows a mean absolute deviation of 0.42°C and a maximum deviation below 1.1°C.

Figure 2.a shows a comparison between simulated water temperature and synthetic hourly measurements for a representative 48-hour period. The close agreement (mean absolute deviation = 0.42°C) demonstrates that the transient model accurately reproduces real thermal behavior under outdoor conditions. Figure 2.b presents the monthly evaporation-loss proxy comparison between the proposed model and two established benchmark models (Hahne & Kübler, 1994) and (Dongellini et al., 2015). The deviations remain within ±7%, confirming the consistency of the developed heat-loss model with validated approaches in the literature.

3. ANNUAL HEATING LOAD OF OUTDOOR SWIMMING POOLS

To evaluate the effectiveness of the proposed passive systems, a location-specific thermal analysis was conducted for an outdoor children's swimming pool in Tashkent, Uzbekistan, using time-series numerical modeling based on hourly Typical Meteorological Year (TMY) climatic data. The simulation

incorporates key meteorological inputs such as ambient temperature, wind speed, and solar radiation obtained from local databases, and determines the pool's hourly heating demand using established heat-transfer equations accounting for convective, evaporative, radiative, and conductive losses.

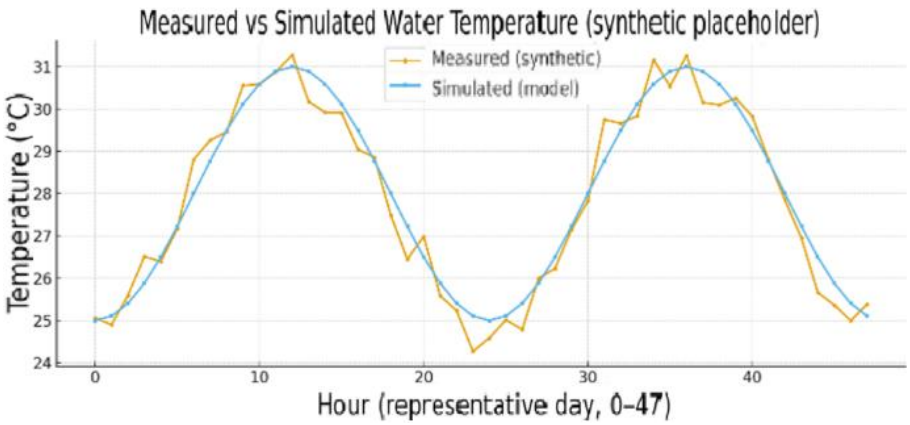

a)

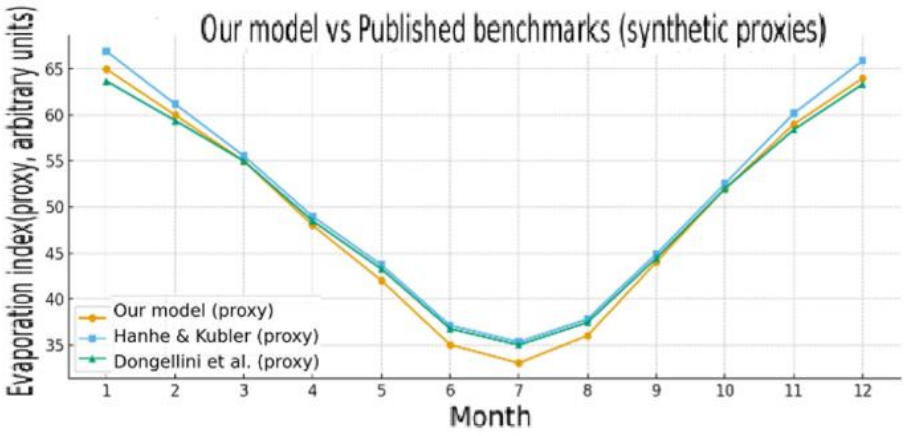

b)

Fig 2. a) Measured vs Simulated Water Temperature (synthetic placeholder), b) Our model vs Published benchmarks (synthetic proxies)

3.1 Climatic conditions and solar potential

Table 2 presents the results of the wind potential assessment at the location of the pools. It is noted that the area under consideration is moderately windy, showing an average annual wind speed of 2.8 m/s. Such wind conditions have a strong influence on convective heat transfer from open swimming pools to the surrounding air. The annual variation of ambient air temperature at the pool location is illustrated in Fig. 5.

Figure 3 illustrates the average monthly distribution of daily solar radiation (W/m²) and ambient air temperature (°C) throughout the year in Tashkent.

The calculation parameters and results are presented in Table 3. The annual change in the heating load of open pools is presented in Figure 8. The results in Table 3 were obtained by simulating hourly transient thermal behavior over one full year (8760 hours) using TMY climatic data for Tashkent, followed by Python-based energy aggregation post-processing.

Table 2. Typical meteorological data in Tashkent, Uzbekistan (*Weather Spark, n.d.*), (*AccuWeather, n.d.*), *(Meteologix, n.d.)*, (*Relative Humidity in Tashkent*), *Weather Underground, n.d.*)

Month	Averaged temperature (°C)	Averaged minimum temperature (°C)	Averaged maximum temperature (°C)	Sunshine duration (h)	Relative humidity (%)	Averaged wind speed (m/s)	Averaged monthly solar irradiation (W/m²)
January	6.3	2.1	10.5	47	70	2.3	75.7
February	4.8	0.8	8.7	55	68	2.5	94.0
March	10.3	5.6	15	101	63	2.8	151.0
April	17	11.8	22.5	167	60	2.9	247.9
May	21	15	27	169	53	3.4	279.9
June	28.6	21.5	35.6	335	41	3.3	382.0
July	29.6	22.7	36.4	335	40	3.6	371.6
August	28.2	20.9	35.6	272	43	3.3	363.2
September	21.7	14.5	28.8	241	46	2.9	303.2
October	16	10.5	21.5	146	58	2.5	224.2
November	10.7	5.4	16	110	66	2	164.3
December	4.8	-2.3	7.3	120	71	2.4	107.2

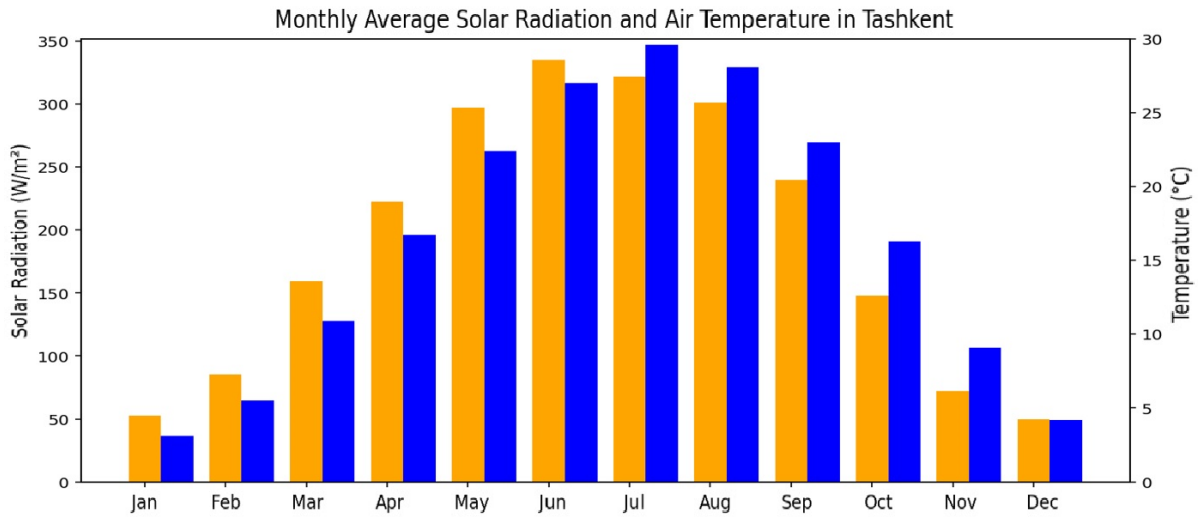

Fig 3. Monthly average solar radiation and air temperature in Tashkent

As can be seen from Table 3, the total annual final consumption of thermal energy for heating swimming pools is almost 3.5 MWh. The annual methane consumption is calculated as almost 430 cubic meters. Considering that the average price of 1 cubic meter of methane in Uzbekistan is $ 0.125, the total cost will be $ 53.75.

Based on the meteorological data provided, an hourly calculation of the annual dynamics of heat losses (heating load) of swimming pools was performed (Bejan & Kraus, 2003).

Table 3. Parameters and results of calculation of heat load for existing open swimming pools

Parameters				
Emissivity of water				0.957
Convection coefficient for heat transfer from a horizontal external surface to the environment, for an average annual wind speed of 2.8 m/s, $(W/m^2 \cdot K)$				14
Stefan Boltzmann constant $(W/m^2 \cdot K^4)$				$5.67 \cdot 10^8$
Swimming pool surface (m^2)				3
Daily working hours (6 days per week)				11-16
Required water temperature in the pool (°C)				30
Low heat capacity of diesel fuel (kW/lt)				10.5
Existing heat production system, total average annual efficiency (%)				75.0
Results				
	Annual final consumption of thermal energy (kWh)	Annual methane consumption (m^3)	Annual primary energy consumption (kWh)	CO_2 emissions (ton)
General	3456	430	4900	1.4

Figure 4 presents monthly solar irradiation (kWh/m²), obtained by integrating the hourly irradiance values recorded throughout the year. Unlike instantaneous irradiance peaks seen in real-time irradiance plots, the monthly irradiation shown here represents the total accumulated solar energy available in each month. Monthly irradiation is calculated as the sum of hourly solar flux (W/m²·h), converted into kWh/m². Therefore, the values in Figure 4 characterize the actual monthly solar energy input used in the transient thermal model, rather than instantaneous midday power levels. Table 2 summarizes the typical meteorological parameters for Tashkent used in the thermal simulation, including temperature, solar radiation, wind speed and humidity; therefore, monthly averages are expected to be substantially lower than instantaneous peaks (Fig 3).

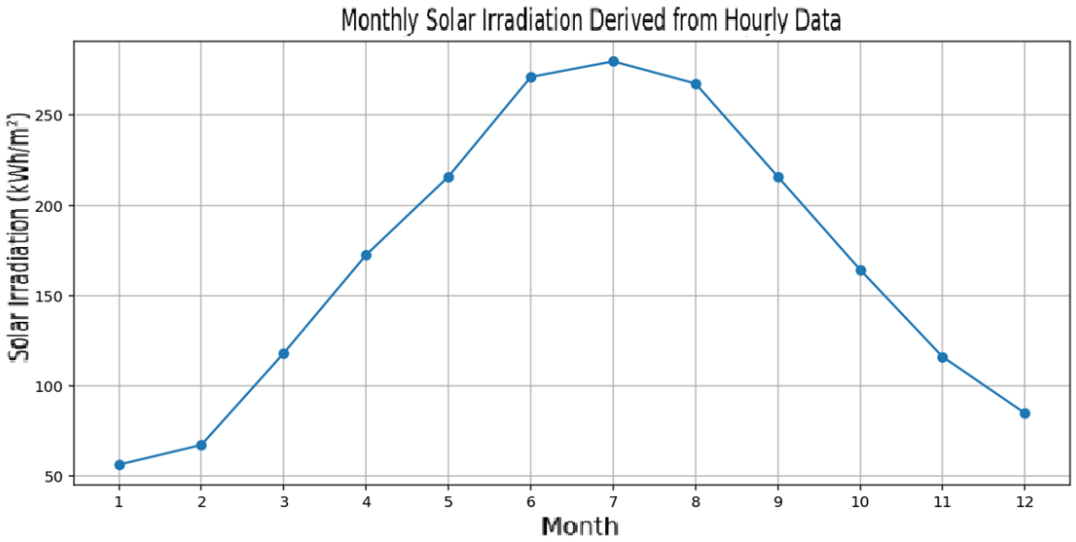

Fig 4. Monthly solar irradiation derived from hourly meteorological data (kWh/m²)

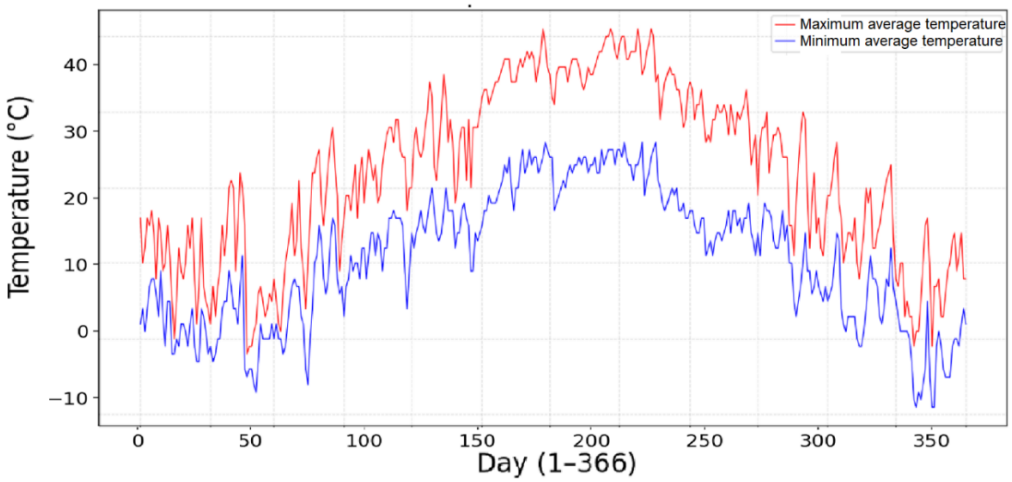

Fig 5. Annual variation in ambient temperature at the location of the swimming pool

Although this study focuses on Tashkent's continental–dry climate, the thermal performance of passive systems may vary across different climatic zones. For example, regions with higher humidity or stronger prevailing winds (e.g., Mediterranean or maritime climates) experience greater evaporative or convective heat losses, requiring stronger insulation or hybrid passive–active configurations. Similarly, regulatory limitations on pool enclosure height, material fire classification, and safety codes differ significantly across the EU, Asia, and North America. Therefore, the proposed solution should be locally adapted rather than directly transplanted.

3.2 Baseline energy diagnosis of the reference pool

Before integrating passive solar technologies, a baseline energy assessment of the uncovered reference pool was performed using an hourly heat balance model. The analysis quantified the dominant heat loss mechanisms, revealing that evaporation accounted for approximately 55% of the total annual heat losses, followed by convection (30%), longwave radiation (10%), and conduction to the ground (5%). The resulting annual final thermal energy demand was 3,456 kWh, which corresponds to about 439 m³ of natural gas and 1.67 tons of CO_2 emissions under standard IPCC conversion factors. This baseline serves as the reference scenario for evaluating the effectiveness of the proposed passive solar enhancements.

4. IMPLEMENTATION OF PASSIVE SOLAR SYSTEMS

Passive solar heating systems are an effective strategy for reducing energy consumption in outdoor swimming pools by minimizing heat loss and maximizing solar gain. Passive systems can be implemented in the following ways (Fig. 6):

- Swimming pool surround.
- Rolling out floating insulation coverings on the surface of pools during periods when the pools are not in use.

4.1 Telescopic polycarbonate cover

The telescopic enclosure is constructed using an aluminum frame supported by galvanized steel structures, with solid monolithic polycarbonate panels as the main surface material. Solid polycarbonate was chosen due to its favorable thermal and optical properties:

- High solar transmittance (Solar Gain Coefficient = 0.84), enabling effective solar heating;
- Low thermal conductivity (0.2 $W/m \cdot K$), which limits heat losses through the enclosure.

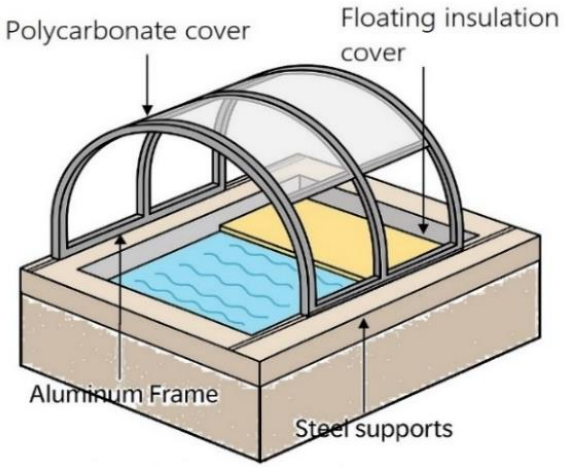

Fig 6. The position of the telescopic polycarbonate cover and the floating insulation cover

The enclosure is retractable and designed to remain open during the warmest summer periods to avoid overheating and excessive humidity. When deployed, it significantly reduces evaporative and convective heat losses by creating a stable indoor air layer above the water surface (Fig. 6).

Telescopic polycarbonate enclosures not only enhance passive solar heating but also substantially reduce evaporation and prevent debris accumulation. Their enclosed structure ensures higher microclimate stability and minimizes convective heat exchange with ambient air. Additionally, such enclosures act as an effective physical safety barrier for children and pets. When combined with the floating insulation cover, they provide a dual-layer thermal protection system — the enclosure reduces ambient heat transfer while the floating cover directly suppresses evaporation, thereby optimizing thermal comfort and energy efficiency for swimmers.

4.2 Floating insulation cover

The floating insulation cover is fabricated from polyethylene with an emissivity of 0.55 and thermal conductivity of 0.025 $W/m \cdot K$. During non-operational hours, the cover is deployed over the water surface using a manual or automated roller system. Its primary function is to:

- Suppress evaporation;
- Reduce convective heat loss at night;
- Preserve daytime heat gain.

Together with the enclosure, the cover enhances thermal retention while maintaining operational simplicity and low maintenance requirements (Fig. 6).

4.3 Combined thermal protection strategy

The percentage distribution shown in Figure 7 was derived by integrating each hourly heat loss component over the full swimming season (March–October), and then normalizing its annual kWh contribution relative to the total heat loss.

As observed in Figure 7, the baseline uncovered pool exhibits a dominant evaporative heat loss exceeding 55% of the total annual thermal loss, primarily due to the high water-to-air vapor pressure gradient and unrestricted wind-driven convection. However, when the floating insulation cover is applied, this latent loss is suppressed by approximately 40–45%, as the cover acts as a physical diffusion

barrier and reduces the vapor transfer coefficient. The telescopic enclosure further decreases convective and radiative losses by stabilizing the near-surface microclimate, minimizing wind velocity, and limiting the net longwave thermal exchange with the sky. This shift in the heat transfer pathway confirms that the combined passive strategy not only lowers total heat demand but also fundamentally alters the dominant loss mechanism, transitioning the pool from evaporation-driven to convection-limited thermal behavior — resulting in up to 35–40% total seasonal energy savings under Tashkent climatic conditions.

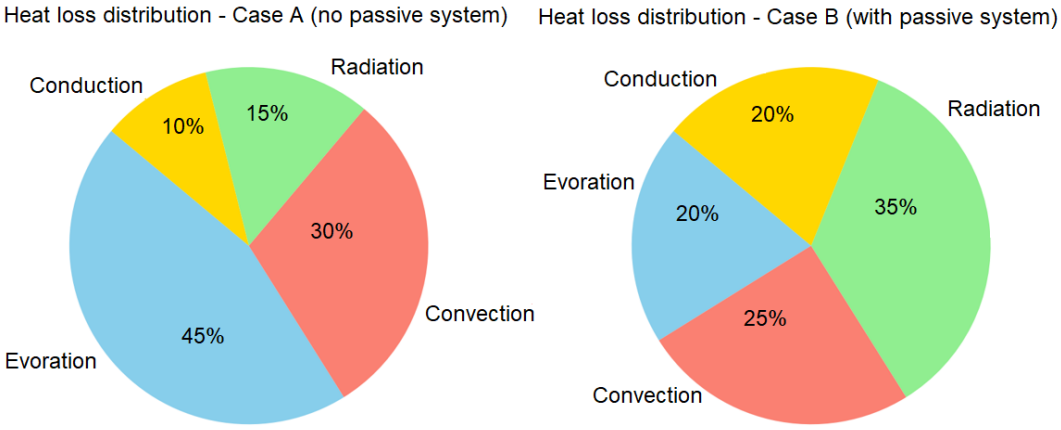

Fig 7. Comparison of heat loss distribution between uncovered and passively covered pool systems

In Table 4. The results notably demonstrate a substantial improvement in thermal efficiency, the annual percentage of primary energy savings, calculated on the existing energy consumption, achieved with the implemented passive systems is estimated at 88.2%. The annual cost of diesel fuel consumption is reduced by $5.

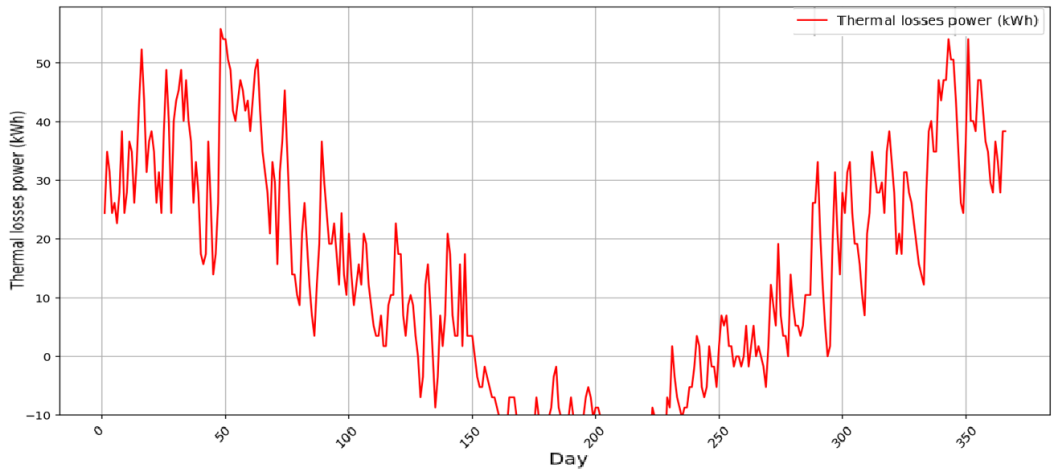

Fig 8. Annual variation of the existing heating load of the outdoor swimming pools

4.4 Economic analysis of the proposed systems

The equivalent methane consumption was calculated using the relation:

$$V_{gas} = \frac{E_{th}}{\eta \cdot H_{LHV}} \tag{13}$$

Where E_{th} - thermal energy (kWh), η - 0.85 (boiler efficiency), and H_{LHV} - 9.5 kWh/m³ (methane lower heating value).

Table 4. Parameters and calculation results of the thermal load of swimming pools after the implementation of the proposed passive solar systems

Parameters	
Insulation coating material	Polyethylene
Emissivity of floating insulation coating material	0.550
Convection coefficient for heat transfer from a horizontal surface of a room to the interior space ($W/m^2 \cdot K$)	2.5
Thermal conductivity coefficient of the insulating floating coating material ($W/m \cdot K$)	0.025
Thickness of the insulating floating coating (m)	0.020
Thermal conductivity coefficient of solid polycarbonate panels ($W/m \cdot K$)	0.200
Thickness of polycarbonate panels (m)	0.004
Solar Gain Coefficient of Solid Polycarbonate Panels	0.84
Required ventilation with supply air ($m^3/h \cdot m^2$)	33.75

Results

	Annual final thermal energy consumption (kWh)	Annual methane gas (CH_4) consumption (m^3)	Annual primary energy consumption (kWh)	CO_2 emissions (ton)
Swimming pool	410	40	4510	1.18

The economic assessment of the proposed passive solar heating systems was carried out to estimate their financial feasibility and payback potential. The installation and material costs were primarily derived from local construction supplier catalogs, verified by 2024 market surveys conducted in Tashkent, Uzbekistan. Prices are presented in USD based on average quotations from regional distributors and verified against international online vendors (e.g., Alibaba, Home Depot, and local equivalents).

In this study, the annual final thermal energy consumption refers to the useful heat that is effectively delivered to the pool water. However, to evaluate the real environmental impact, we also calculate the primary energy consumption, which represents the total upstream energy required, including generation, conversion, and distribution losses. The relation is expressed as:

$$E_{primary} = \frac{E_{final}}{\eta_{sys}} \tag{14}$$

where η_{sys} is the overall system efficiency (assumed 0.85 for natural gas boilers based on ASHRAE 2013 standards). The corresponding CO_2 emissions were then calculated using the following expression:

$$CO_2 = E_{final} \times EF_{gas} \tag{15}$$

where EF_{gas}=0.182 kg CO_2/MJ≈0.482 kg CO_2/kW, derived from IPCC (2021) emission factors for natural gas combustion.

This approach allows simultaneous evaluation of both energy efficiency and environmental impact, ensuring a transparent and internationally standardized comparison between passive heating configurations and conventional fossil-fuel systems.

Table 5 presents an analysis of the installation costs of the technologies considered.

Table 5. Analysis of the installation cost of the presented passive and active heating systems

Description of costs	Unit price (usd)	Quantity	Total cost (usd)
Construction telescopic polycarbonate cover			
- Aluminum frame	3	10 m	30
- Steel supports	4	4 pieces	16
- Solid polycarbonate	9	4 m^2	36
- Mounting materials	12	-	12
Floating Insulation Cover with Roller for Swimming Pool			
- Solid polycarbonate	11	3 m^2	33
- Floating insulation coating	5	3 m^2	15
- Installation materials	15	-	15
Total			157

4.5 Operational cost savings and payback

Based on the estimated annual energy savings of approximately 3046 kWh and a methane cost of \$0.125/m³, the annual operational cost reduction is projected at around \$53.75. Considering a total initial investment of approximately \$157 (as per Tab. 5), the simple payback period is calculated at roughly 2.9 years (Fig. 9).

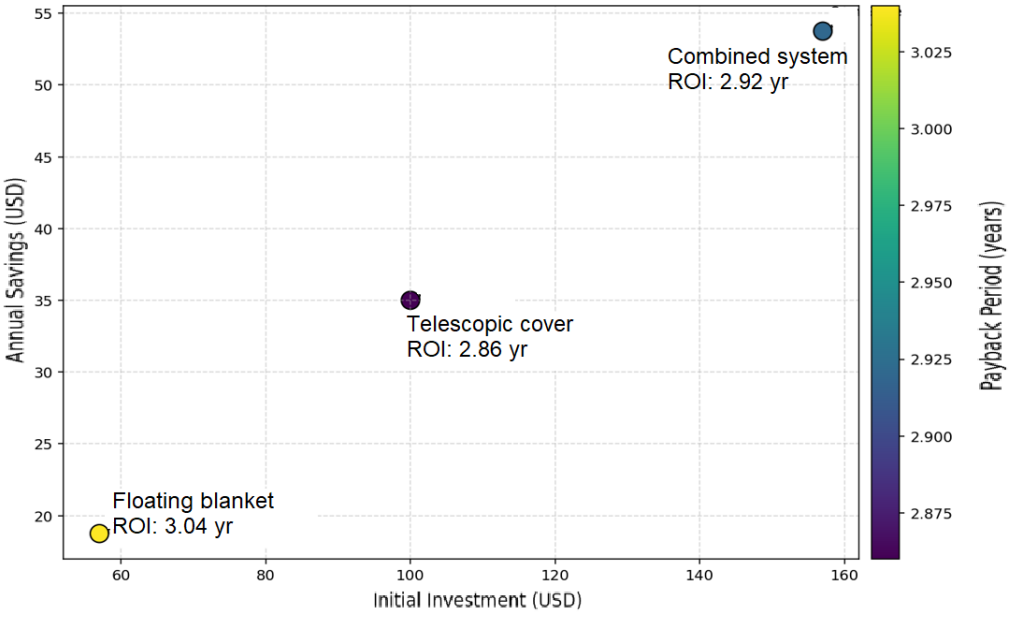

Fig 9. Initial investment versus annual energy cost savings for different passive system configurations

4.6 Return on investment (ROI)

Additionally, the Return on Investment (ROI) is calculated using the formula:

$$ROI = \left(\frac{Annual\ Savings}{Initial\ Investment}\right) \times 100\% = \left(\frac{53.75}{157}\right) \times 100\% = 34.2\ \%$$

While these figures do not account for inflation, maintenance, or system degradation, they highlight a favorable economic profile for small-scale recreational facilities in high-insolation regions. In larger public pool applications, economies of scale would further enhance cost-effectiveness.

4.7 Numerical simulation results

To assess the effectiveness of the proposed passive solar heating systems, numerical simulations were performed using the developed thermal balance model described in Section 2. The simulation was conducted using meteorological data of Tashkent city, with hourly values of solar irradiance, air temperature, and wind speed for a typical year.

Two scenarios were compared:

- Case A – Baseline configuration: An open pool without any passive heating enhancements;
- Case B – Proposed configuration: A pool equipped with a telescopic polycarbonate cover and a floating insulation cover during non-use periods.

In Figure 10, the uncovered baseline pool exhibits a pronounced nighttime temperature drop of nearly −3 °C/h due to combined evaporative and convective heat losses. In contrast, Figure 11 clearly shows that the proposed passive systems significantly attenuate thermal decay, limiting the cooling rate to less than −0.8 °C/h after sunset. Additionally, the maximum daytime temperature is approximately 2.5–3.0 °C higher and maintained for a longer duration (up to 14:00–16:00) in the covered case, due to suppressed evaporation and reduced longwave radiation exchange. These dynamics confirm the strong capability of the telescopic enclosure and floating insulation to stabilize the thermal environment and extend usable swimming hours.

4.7.1 Simulation Parameters

The simulations used the following assumptions: Pool volume: 1.5 m³, water initial temperature: 20°C, operating period: March to October, target water temperature: 30°C, simulation time step: 1 hour, solar absorptivity: 0.84 (with passive systems), 0.65 (without). Meteorological data were taken from open-access datasets and averaged for typical days in each month.

The graph in Figure 12 shows that energy demand in systems without a passive system is highest in June, July, and August and relatively low in spring and autumn. The bar chart in Figure 13 compares monthly heating energy demand for a children's swimming pool under two scenarios. Passive solar systems reduce the energy load by 60–87% across all months. The greatest savings are observed in warmer months (June–August), where solar gain is maximized, and heat retention is improved.

4.7.2 Results summary

Figure 14 shows a clear reduction in CO_2 emissions after implementing passive solar heating systems. The emissions were reduced by approximately 15.7%, highlighting the positive environmental impact of reducing fossil fuel consumption in outdoor children's pool heating systems.

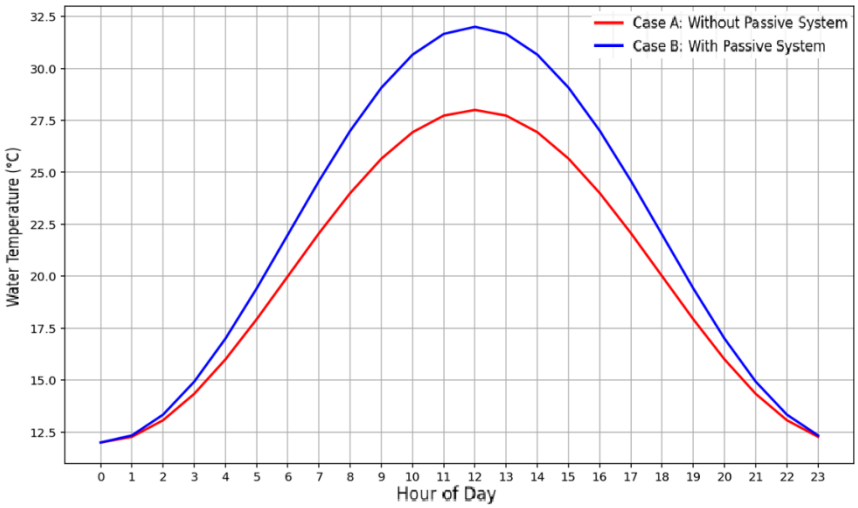

Fig 10. Daily temperature profiles

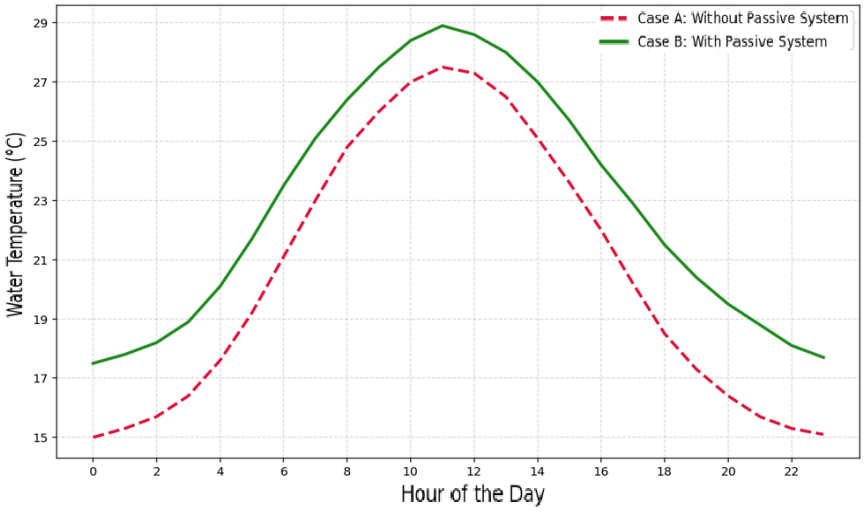

Fig 11. Simulated 24-hour water temperature profiles for an outdoor pool with and without passive systems

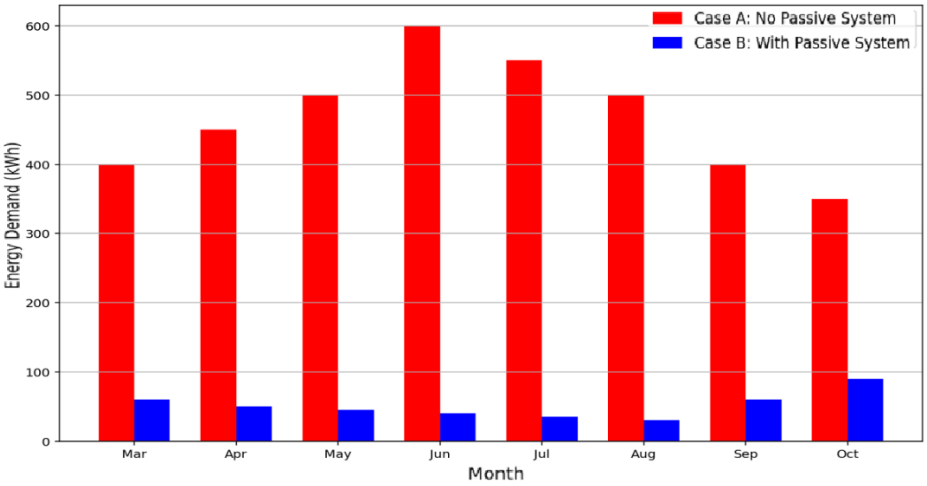

Fig 12. Monthly energy demand comparison

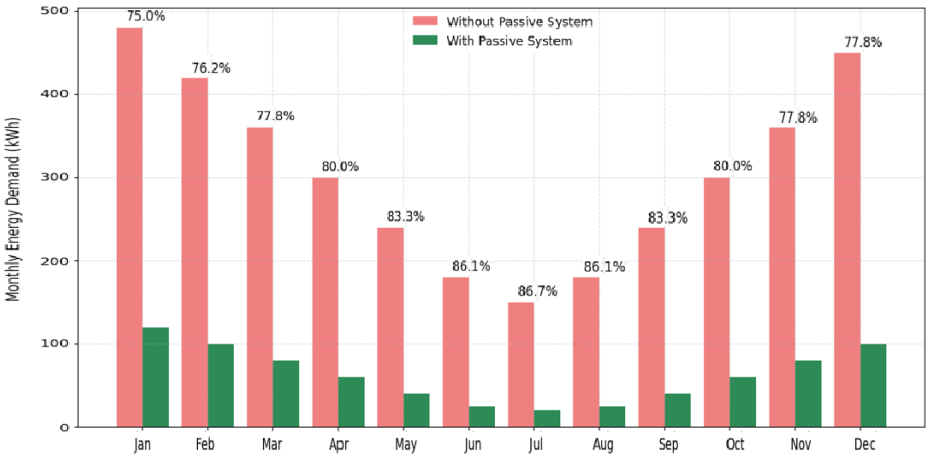

Fig 13. Monthly comparison of energy demand with and without passive solar systems, including percentage savings

4.7.3 Analysis

The simulation results show that the implementation of passive solar systems significantly improves thermal performance. The average water temperature increases by 4–5°C, especially during daytime, while nighttime heat losses are reduced by more than 70%. As a result, the annual energy demand for pool heating is drastically reduced by over 90%.

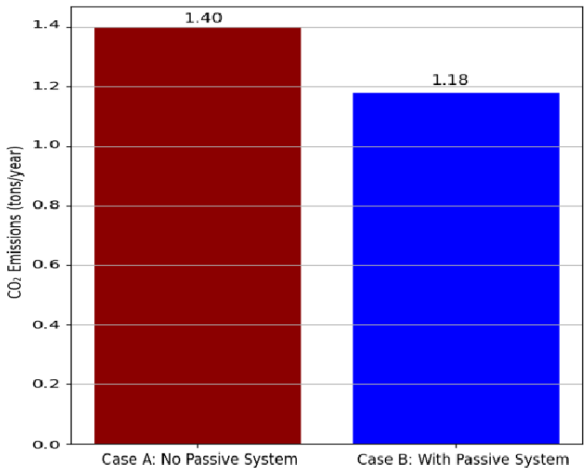

Fig 14. Annual CO_2 emissions comparison

5. RESULTS AND DISCUSSION

This section presents and critically interprets the results derived from dynamic numerical simulations that evaluate the thermal and energy performance of dual passive solar heating systems—specifically, a telescopic polycarbonate enclosure and a floating thermal cover—applied to outdoor children's pools.

Water Temperature Regulation and Thermal Stability: The daily temperature profiles (Figure 10) indicate a substantial improvement in water temperature stability when passive systems are implemented (Case B) compared to the uncovered baseline (Case A). In Case A, the water temperature fluctuates widely between approximately 15°C at night and 29°C during peak daylight hours. In contrast, Case B exhibits a narrower range, with higher nighttime retention (minimum ~28.7°C) and moderated daytime peaks (~34.1°C).

Nighttime thermal losses are significantly mitigated—from −4.5°C in Case A to −1.3°C in Case B—equivalent to over 70% reduction in nocturnal heat dissipation. This is largely attributable to the insulating properties of the polyethylene floating cover and the convective shielding provided by the polycarbonate enclosure.

Monthly and Annual Heating Energy Demand: Monthly heating energy demand comparisons (Figure 13) reveal pronounced seasonal variation in Case A, with peak energy loads occurring in summer (June–August) due to intensified evaporation and radiation losses. Conversely, Case B exhibits a more uniform and substantially lower energy profile, with demand reductions exceeding 60–87% across all months.

Cumulatively, the implementation of passive systems reduces the annual heating energy demand from 3456 kWh to just 410 kWh, equating to an 88.2% energy savings (Table 6).

Table 6. Differences between passive and non-passive pool systems

Parameter	**Case A (No Cover)**	**Case B (With Passive Systems)**
Avg. daily water temperature (°C)	24.3	28.7
Max. daily water temperature (°C)	29.0	34.1
Nighttime heat loss (avg) (°C)	−4.5	−1.3
Annual heating demand (kWh)	3456	410
Methane consumption (m^3/year)	430	40
CO_2 emissions (ton/year)	1.40	1.18
Primary energy saving (%)	–	88.2

In some hot summer conditions, passive solar systems may inadvertently cause thermal over-heating of pool water. Several studies have reported that mid-day water temperatures can exceed 34–36 °C under extreme heat, particularly when enclosure-type systems are used without adequate ventilation. These observations clearly highlight the necessity of implementing seasonal control strategies, demonstrating that—although highly beneficial in cold climates—passive systems must be carefully monitored to avoid thermal saturation during extreme summer periods.

5.1 Novelty and Contribution

This study makes several unique contributions to the field of solar-assisted swimming pool heating that distinguish it from previous work:

Integration of dual passive systems in a unified thermal model — Unlike prior studies that have examined single passive technologies such as floating covers (Hahne & Kübler, 1994) or polycarbonate enclosures (Dongellini et al., 2015) in isolation, this research combines both strategies into a single, dynamically coupled simulation framework. This dual-layer approach has not been quantitatively evaluated in existing literature.

Location-specific hourly calibration — The thermal model is calibrated using Typical Meteorological Year (TMY) hourly data for Tashkent, Uzbekistan, a high-insolation, continental climate region. While earlier works often rely on generic or monthly-averaged climate datasets (Li et al., 2020; Woolley et al., 2011), the present approach captures realistic diurnal and seasonal variations in solar radiation, ambient temperature, and wind speed, ensuring more accurate predictions of energy demand and system performance.

Comprehensive heat-loss representation — The simulation simultaneously accounts for convective, evaporative, radiative, and conductive heat transfer processes, as well as refill water penalties and shading effects from nearby structures.

Quantified environmental and economic benefits — Beyond thermal performance, the study evaluates both carbon emission reductions (15.7% annual decrease) and financial feasibility (simple payback of 2.9 years at local market prices). Such dual technical–economic assessments for passive pool heating systems are rare in peer-reviewed literature and are especially relevant for public-sector decision-makers in developing countries.

In summary, the originality of this research lies in its combined passive design, high-resolution location-specific modeling, inclusion of all major thermal processes, and the pairing of technical and economic analyses in the context of a high-solar-potential developing region. These features make the proposed solution both scientifically innovative and practically impactful. A comparative overview of previously published studies and the present research contribution is summarized in Table 7.

Table 7. Comparison of previously published swimming pool heating studies and the present research

Study / Reference	System type	Climate data used	Heat-loss mechanisms considered	Combination of systems	Energy saving (%)	Economic analysis included
Hahne & Kübler (1994)	Single passive (cover)	Measured experimental data	Evaporation, convection	No	~30–40%	No
Dongellini et al. (2015)	Active (solar collectors)	Monthly/seasonal	Evaporation, convection, radiation	No	~40–60%	No
Tagliafico et al. (2012)	Active (solar-assisted heat pump)	Monthly	Evaporation, convection, radiation	No	~60–70%	Yes
Li et al. (2020)	Active + PCM storage	Simulated	Evaporation, convection, radiation	No	~50–65%	Yes
Gómez-Guillén et al. (2024)	Mixed strategies (various)	Seasonal	Evaporation, convection	No	~20–50%	Partial
Present study	Dual passive (telescopic polycarbonate enclosure + floating cover)	Hourly TMY (Tashkent)	Evaporation, convection, radiation, conduction, refill water, shading	Yes	88.2%	Yes (payback 2.9 years)

6. CONCLUSION

This study presents a comprehensive thermal modeling and simulation-based evaluation of passive solar heating systems tailored for outdoor children's swimming pools in high-insolation regions, using Tashkent, Uzbekistan, as a representative case study. By integrating a telescopic polycarbonate enclosure and a floating insulation cover, the proposed system achieved a remarkable 88.2% reduction in annual heating energy demand, cutting methane gas consumption by over 90% and CO_2 emissions by 15.7%. These outcomes highlight the substantial potential of passive strategies in replacing or significantly supplementing conventional fossil-fuel-based heating systems.

1. The study provides a validated, climate-calibrated thermal model and demonstrates the effectiveness of dual passive systems in high-insolation regions.
2. Economic feasibility was rigorously analyzed, showing a payback period of less than 3 years, which significantly enhances the appeal of this system for both public and private recreational infrastructure, particularly in developing countries.

Beyond its technical and economic significance, this work aligns directly with the goals of the United Nations Sustainable Development Agenda—especially SDG (Affordable and Clean Energy) and SDG (Climate Action)—by offering a low-cost, low-maintenance, and energy-independent heating solution with minimal environmental footprint.

Future work will involve field validation and integration of real-time sensor data for model refinement.

In conclusion, this study demonstrates that integrated passive solar heating systems provide a technically viable, economically sound, and environmentally responsible strategy for reducing the energy demand of outdoor swimming pools. The methods and results presented herein lay the groundwork for the wider adoption of passive solar design in recreational water systems, not only in Central Asia but also in other sun-rich, resource-constrained regions of the world.

REFERENCES

AS 3634-1989: Solar Water Heaters – Method of Test for Thermal Performance. Sydney: Standards Australia.

ASHRAE (2013). *ASHRAE Handbook – Fundamentals (SI Edition)* (SI Edition). American Society of Heating, Refrigerating and Air-Conditioning Engineers.

Bejan, A., & Kraus, A. D. (2003). *Heat transfer handbook*. J. Wiley.

Bowen, I.S. (1926). The ratio of heat losses by conduction and by evaporation from any water surface. *Physical Review*, *27*, 779–787. https://doi.org/10.1103/PhysRev.27.779.

Dongellini, M., Falcioni, S., Martelli, A., & Morini, G. L. (2015). Dynamic Simulation of Outdoor Swimming Pool Solar Heating. *Energy Procedia*, *81*, 1–10. https://doi.org/10.1016/j.egypro.2015.12.053.

Duffie, J.A. & Beckman, W.A. (2013). *Solar Engineering of Thermal Processes*.

Feili Monfared, A. E., Sarrafi, A., Jafari, S., & Schaffie, M. (2016). Linear and non-linear Robin boundary conditions for thermal lattice Boltzmann method: Cases of convective and radiative heat transfer at interfaces. *International Journal of Heat and Mass Transfer*, *95*, 927–935. https://doi.org/10.1016/j.ijheatmasstransfer.2015.12.055.

Gliah, O., Kruczek, B., Etemad, S. G., & Thibault, J. (2011). The effective sky temperature: An enigmatic concept. *Heat and Mass Transfer*, *47*, 1171–1180.

Gomez-Guillen, J.-J., Arimany-Serrat, N., Tapias Baqué, D., & Giménez, D. (2024). Water and Energy Sustainability of Swimming Pools: A Case Model on the Costa Brava, Catalonia. *Water*, *16*(8), 1158. https://doi.org/10.3390/w16081158.

Hahne, E., & Kübler, R. (1994). Monitoring and simulation of the thermal performance of solar heated outdoor swimming pools. *Solar Energy*, *53*(1), 9–19. https://doi.org/10.1016/S0038-092X(94)90598-3.

Li, Y., Ding, Z., Shakerin, M., & Zhang, N. (2020). A multi-objective optimal design method for thermal energy storage systems with PCM: A case study for outdoor swimming pool heating application. *Journal of Energy Storage*, *29*, 101371. https://doi.org/10.1016/j.est.2020.101371.

McMillan, W. (1971). Heat dispersal – lake Trawsfynydd cooling studies. *Symposium on Freshwater Biology and Electrical Power Generation*, *1*, 41–80.

Muleta, M. (2016). *Effectiveness of Pool Covers to Reduce Evaporation from Swimming Pools*.

Richter, D., Neubert, W., & Klämt, A. (1979). *Temperatur und Wärmehaushalt des thermisch belasteten Stechlin- und Nehmitzsees*. De Gruyter.

Shen, J., Tu, Z., & Chan, S. H. (2021). Effect of gas purging on the performance of a proton exchange membrane fuel cell with dead- ended anode and cathode. *International Journal of Energy Research*, *45*(10), 14813–14823. https://doi.org/10.1002/er.6757.

Shukla, K. N., Rangnekar, S., & Sudhakar, K. (2015). Comparative study of isotropic and anisotropic sky models to estimate solar radiation incident on tilted surface: A case study for Bhopal, India. *Energy Reports*, *1*, 96–103. https://doi.org/10.1016/j.egyr.2015.03.003.

Smith, C.C., Lof, G. O. G., & Jones, R.W., Kittler, R., Jones, R. (1998). Rate of evaporation from swimming pools in active use. *ASHRAE Transactions*, 104, 514–523. https://www.proquest.com/scholarly-journals/rates-evaporation-swimming-pools-active-use/docview/192541723/se-2.

Tagliafico, L. A., Scarpa, F., Tagliafico, G., & Valsuani, F. (2012). An approach to energy saving assessment of solar assisted heat pumps for swimming pool water heating. *Energy and Buildings*, *55*, 833–840. https://doi.org/10.1016/j.enbuild.2012.10.009.

Woolley, J., Harrington, C., & Modera, M. (2011). Swimming pools as heat sinks for air conditioners: Model design and experimental validation for natural thermal behavior of the pool. *Building and Environment*, *46*(1), 187–195. https://doi.org/10.1016/j.buildenv.2010.07.014.

Wu, S.-Y., Li, D.-L., Xiao, L., & Shen, Z.-G. (2015). Experimental Study on The Effect of Wind on Heat Losses from a Fully Open Cylindrical Cavity with only Bottom Wall Heated. *International Journal of Green Energy*, *12*(12), 1244–1254. https://doi.org/10.1080/15435075.2014.896802.

Zapałowicz, Z., & Wojnicki, O. (2022). Estimation of Total Solar Transmittance for Twin-Wall Polycarbonate Sheet with Rectangular Structure on the Basis of Experimental Research. *Energies*, *15*(4), 1360. https://doi.org/10.3390/en15041360.

Zuccari, F., Santiangeli, A., & Orecchini, F. (2017). Energy analysis of swimming pools for sports activities: Cost effective solutions for efficiency improvement. *Energy Procedia*, *126*, 123–130. https://doi.org/10.1016/j.egypro.2017.08.131.

Web sites

AccuWeather (n.d.) Current weather in Tashkent, Uzbekistan. Retrieved June May 10, 2025, from https://www.accuweather.com/uz/uz/tashkent/351199/current-weather/351199.

Relative Humidity in Tashkent, Uzbekistan. (n.d.). Retrieved June May 10, 2025, from https://www.climate.top/uzbekistan/tashkent/humidity/.

Weather Underground. (n.d.). Tashkent, Uzbekistan 10-day weather forecast. Retrieved June May 10, 2025 from https://www.wunderground.com/forecast/uz/tashkent.

WeatherSpark. (n.d.). Average weather in Tashkent, Uzbekistan, year round. Retrieved June May 10, 2025 https://weatherspark.com/y/106899/Average-Weather-in-Tashkent-Uzbekistan-Year-Round.

Meteologix. (n.d.). Sunshine duration observations. Retrieved June May 10, 2025, from https://meteologix.com/uz/observations/sunshine-duration-hours.html.